J. Biochem. 2011;149(5):539–550 doi:10.1093/jb/mvr012

JB THE JOURNAL OF BIOCHEMISTRY

Biochemical characterization of the novel rice kinesin K23 and its kinetic study using fluorescence resonance energy transfer between an intrinsic tryptophan residue and a fluorescent ATP analogue

Received October 14, 2010; accepted January 4, 2011; published online January 28, 2011

Nozomi Umezu[1], Nobue Hanzawa[2], Masafumi D. Yamada[2], Kazunori Kondo[2], Toshiaki Mitsui[3] and Shinsaku Maruta[1,2,*]

[1]Division of Bioengineering, Graduate School of Engineering; [2]Department of Bioinformatics, Faculty of Engineering, Soka University, Hachioji, Tokyo 192-8577; and [3]Laboratories of Plant and Microbial Genome Control, Graduate School of Science and Technology, Niigata University, Niigata 950-2181, Japan

*Shinsaku Maruta, Department of Bioinformatics, Faculty of Engineering, Soka University, Hachioji, Tokyo 192-8577, Japan. Tel: +81 426 91 9443, Fax: +81 426 91 9312, email: maruta@soka.ac.jp

We previously demonstrated that the rice kinesin K16, which belongs to the kinesin-7 subfamily, has unique enzymatic properties and atomic structure within key functional regions. In this study, we focused on a novel rice plant kinesin, K23, which also belongs to the kinesin-7 subfamily. The biochemical characterization of the K23 motor domain (K23MD) was studied and compared with the rice kinesin K16 and other related kinesins. K23 exhibits ~45-fold (1.3 Pi mol^{-1}site mol^{-1}s^{-1}) lower microtubule-dependent ATPase activity than conventional kinesins, whereas its affinity for microtubules is comparable with conventional kinesins. MgADP-free K23 is unstable compared with the unusually stable MgADP-free K16MD. The enzymatic properties of K23MD are somewhat different from those of K16. We used a fluorescent ATP analogue 2′(3′)-*O*-(*N*′-methylanthraniloyl)-ATP (mant-ATP) for the kinetic characterization of K23. The fluorescence of mant-ATP was not significantly altered during its hydrolysis by K23. However, significant fluorescence resonance energy transfer (FRET) between mant-ATP and W21 in the motor domain was observed. The kinetic study using FRET revealed that K23 has unique kinetic characteristics when compared with other kinesins.

Keywords: ATP analogue/kinesin/kinetics/plant/rice.

Abbreviations: BSA, bovine serum albumin; CENP-E, centromeric protein E; Co-NTA, cobalt nitrilotriacetic acid; DTT, dithiothreitol; FRET, fluorescence resonance energy transfer; IPTG, isopropyl-β-D-thiogalactopyranoside; KCH, calponin homology domain-containing kinesin; KHC, conventional kinesin heavy chain; KIF, kinesin superfamily protein; Mant-ATP, 2′(3′)-O-(*N*′-methylanthraniloyl)-ATP; MES, 2-(*N*-morpholino)ethanesulphonic acid; MD, motor domain; MOPS, 3-(*N*-morpholino)propanesulphonic acid; MT, microtubule; NBD-ATP, 2′(3′)-O-[6-(*N*-(7-nitrobenz-2-oxa-1,3-diazol-4-yl)-amino)hexanoic]-ATP; PIPES, 1,4-piperazinediethanesulphonic acid; PMSF, phenylmethylsulphonyl fluoride; SDS–PAGE, sodium dodecyl sulphate polyacrylamide gel electrophoresis; TCA, trichloro acetic acid; WT, wild-type.

Kinesins constitute a superfamily of ATP-driven microtubule motor proteins (KIFs) that are found in all eukaryotes. Kinesins perform a diverse range of cellular functions, such as the transport of organelles and vesicles, spindle formation and elongation, chromosome segregation during cell division, microtubule dynamics and morphogenesis (*1–4*). A considerable number of kinesin superfamily members found in animals have been extensively studied, with particular emphasis on members from mice and humans. In contrast, only a few kinesins have been characterized in plants, including those of *Arabidopsis thaliana* (*5–15*).

The first complete DNA sequencing of a plant genome, *Arabidopsis*, led to the identification of 61 kinesin-like genes, which was the largest known number of kinesin genes in a single organism until recently (*16*). In 2004, the complete rice genome sequence was found to code 41 kinesin-like proteins (*17*). Phylogenetic analyses using the motor-domain sequences of the kinesins in these two plants and animals revealed that particular prominent subgroups contain only plant kinesins, including the At1 and At2 subfamilies of kinesin-7 and a subgroup of kinesin-14 (*5*, *15*, *18*). The kinesin-7 family can be subdivided into three subfamilies: CENP-E (centromeric protein E; the original kinesin-7 family, which consists of both animal and plant kinesins), At1 and At2. Both the At1 and At2 subfamilies include only plant kinesins. CENP-E is located at the kinetochore region during mitosis in mammals, and interacts with mitotic checkpoint proteins as part of its role in mitotic progression (*19*).

These plant-specific kinesins possibly participate in plant-specific functions, including the formation of phragmoplasts evident at cell division, morphogenesis of leaf trichomes and flowers, and the rapid movement

Downloaded from http://jb.oxfordjournals.org/ at Changhua Christian Hospital on September 26, 2012

© The Authors 2011. Published by Oxford University Press on behalf of the Japanese Biochemical Society. All rights reserved

of Golgi stacks (*8*, *9*, *12*, *13*). For example, some kinesins of the At1 subfamily regulate the localization of the phragmoplast and are involved in its construction (*7*, *20*). A major difference between animal and plant cell division is that in plant cells a cell plate that spans the middle of the cytoplasm is formed, and new cell walls are formed between the two daughter cells. In contrast, in animal cells a contractile ring pinches the cell in half. A key step in the formation of the cell plate is the generation of the phragmoplast, which is formed at the spindle midzone and contains two opposing sets of microtubules together with actin filaments and Golgi-derived vesicles (*7*, *21*, *22*). The dwarf bamboo shoot 1 (*dbs1*) mutation at the OsNACK1 (LOC_Os01g33040/Os01g0513900) locus encodes a kinesin-7 member and causes severe dwarfism in rice (*7*). OsNACK1 is an orthologue of NACK1 in *Arabidopsis* and tobacco. NACK1 is involved in the localization of a mitogen-activated protein kinase cascade toward the phragmoplast midzone and plays a critical role in microtubule turnover in the phragmoplast (*23*, *24*). The *dbs1* mutant exhibits cell wall stubs in rapidly dividing cells, thereby reflecting defects in cytokinesis (*7*, *23*, *25*).

We previously focused on plant-specific kinesins found in the rice genome. One of these, K16, which belongs to the At2 subfamily, exhibits several unique enzymatic characteristics (*5*, *26*–*28*). The most interesting property of K16 is the high stability of the motor domain (MD) under nucleotide-free conditions, which contrasts with conventional kinesins that are very labile in an ADP-free state (*29*, *30*). Recently, the crystal structure of the K16 motor domain (K16MD) was determined as part of a complex with MgADP (*28*). The overall structure of the K16MD is similar to conventional kinesin motor domain conformations. However, the neck-linker of the K16MD bound to MgADP shows an ordered conformation in a position that is quite different from that observed in conventional kinesin structures. Such a difference may reflect the unique enzymatic characteristics of K16 and be related to currently unknown plant-specific roles.

Furthermore, we characterized the plant-specific rice kinesin, O12, which has a calponin homology (CH) domain that is known to function as an actin binding site. The CH domain-containing kinesins are called 'kinesins with calponin-homology domains' (KCH) that belong to a plant-specific group of kinesin-14, and are thus far found only in rice (at least three genes), *Gossypium hirsutum* (cotton) and *Arabidopsis thaliana* (*9*–*10*, *31*).

In this study, we attempted to characterize a novel kinesin, K23, which belongs to the At1 subfamily of kinesin-7 (*5*). Biochemical analysis revealed that K23 has low ATPase activity and higher affinity for microtubules than other rice kinesins (*26*, *31*). The enzymatic properties of K23 were found to be similar to CENP-E kinesin. This may indicate that similar biochemical properties represent an important feature among kinesin-7 family members. We used fluorescence resonance energy transfer (FRET) between a fluorescent ATP analogue and an intrinsic tryptophan for studying the kinetics of K23. Using this method, K23 was found to have unique kinetic properties when compared to other rice kinesins we have previously characterized.

Materials and Methods

Cloning and in vitro *mutagenesis of the kinesins*

The K23 plasmid (Accession No. AK102262) was supplied by the National Institute of Agrobiological Sciences (NIAS). The DNA fragment encoding the K23 motor domain (amino acids 36–363) was amplified by PCR using the LamdaFLC-K23 plasmid as a template (Prime STAR MAX). The gel-purified PCR products were digested with SalI/EcoRI and ligated into a pET21a vector (TAKARA). The DNA encoding the K23MD W145F/W165F was amplified by PCR using the pET21a::K23MD plasmid. Initially, a set of forward and reverse primers were used for the W145F mutation. The PCR products were self-ligated. Next, a set of forward and reverse primers using the pET21a::K23MD W145F plasmid as the template to introduce the W165F mutation were used. The PCR products were constructed by self-ligation. Thus, a K23 W145F/W165F double-mutation plasmid was made. The DNA encoding the KIF5A motor domain (amino acids 1–334) with a single amino acid mutation, L25W, was amplified by PCR using the pET15b::KIF5AMD plasmid as the template. The PCR products were subsequently self-ligated.

Kinesin expression

The constructed plasmids were transformed into *Escherichia coli* BL21 (DE3) (Invitrogen) for large-scale expression of the recombinant kinesin proteins. Transformations were selected on L-plates with 100 μg ml^{-1} ampicillin. *Escherichia coli* was cultured for 3 h at 37°C at 180 rpm in 2 L L-broth containing 100 μg ml^{-1} ampicillin. For the protein expression of K23MD and its mutant, cultures were induced at an OD_{600} of 0.7–0.8 by adding 0.1 mM isopropyl-β-D-thiogalactopyranoside (IPTG) and 0.1 mM dithiothreitol (DTT). Incubation was continued for 20 h at 18°C. The expression of the KIF5A L25W mutant was induced at an OD_{600} of approximately 0.8 by adding 0.1 mM IPTG and 0.1 mM DTT. Incubation was continued for another 4 h at 37°C. The cells were centrifuged at 5000 rpm for 15 min in a rotor No. 30 (HITACHI Himac CR22G) and subsequently suspended in HEM buffer (10 mM HEPES, pH 7.2, 1 mM $MgCl_2$, 1 mM EGTA, 25 mM NaCl and 1 mM DTT) and stored at −80°C until required.

Purification of rice kinesins

The frozen cells were thawed and suspended in 20 ml sonication buffer [20 mM 3-(*N*-morpholino)propanesulphonic acid (MOPS), pH 7.0, 300 mM NaCl, 1 mM $MgCl_2$, 0.1 mM ATP, 0.2 mM β-mercaptoethanol, 0.5 mM phenylmethylsulphonyl fluoride (PMSF), 2 μg ml^{-1} leupeptin, 1 μg ml^{-1} aprotinin and 1 μg ml^{-1} pepstatin A] and then sonicated for 5 min (5 replicates of 30 s of sonication followed by 1 min on ice) with the micro tip limit set to five and the duty cycle 50% using an Ultras Homogenizer VP-30S (TAITEC, Koshigaya, Saitama). The samples were then centrifuged at 200,000*g* for 1 h. Purification of kinesin K23, its mutants and K16 were carried out according to the methods previously reported using a cobalt nitrilotriacetic acid (Co-NTA) column (*26*, *31*).

Purification and polymerization of tubulin

Tubulin was purified from porcine brain as described by Hackney (*32*, *33*). To polymerize the tubulin in buffer [100 mM 1,4-piperazinediethanesulphonic acid (Pipes), pH 6.8, 1 mM EGTA, 1 mM $MgCl_2$ and 1 mM GTP], the solution was incubated for 30 min at 37°C, and then taxol was added to a final concentration of 10 μM. The taxol-stabilized microtubules (MTs) were pelleted by centrifugation at 200,000 g for 15 min at 37°C (Hitachi Himac CS 120GX), the supernatant was aspirated off and the MT pellet was homogenized in buffer (100 mM Pipes, pH 6.8, 1 mM EGTA, 1 mM $MgCl_2$, 1 mM GTP and 10 μM taxol).

Quantitative determination of protein concentration

The concentration of kinesins samples were determined by the Bradford method using the Coomassie Plus Protein Assay Reagent (Thermo Scientifics, Rockford, IL, USA). The concentration of

Downloaded from http://jb.oxfordjournals.org/ at Changhua Christian Hospital on September 26, 2012

tubulin was determined by the Micro-biuret method established by Itzhaki (*34*).

ATPase assay

ATP in the sample buffer was removed from 1 μM rice kinesin K23MD or 0.1 μM conventional kinesin MD using a Sephadex G-50 fine column (GE) pre-incubated at 25°C for 5 min in 30 mM Tris–HCl (pH 7.5), 3 mM $MgCl_2$, 0.1 mM EDTA, 1 mM EGTA and 1 mM β-mercaptoethanol. For the microtubule concentration dependence assay, microtubule concentrations were 0–20 μM. The NaCl concentration and pH dependence assays were performed in the absence or presence of 5 μM microtubules. The NaCl concentration was 0–300 mM. The following buffers were used for the different pH ranges: pH 4.0–5.0, acetate–NaOH; pH 5.5–6.5, 2-(*N*-morpholino)ethanesulphonic acid (MES)-NaOH; pH 7.0–7.5, MOPS–NaOH; pH 8.0–9.0, Tris–HCl. The addition of 1 mM ATP initiated the ATPase reaction. The ATPase activities of kinesins were terminated by the addition of 10% trichloro acetic acid (TCA). The released P_i was measured using the method outlined by Youngburg and Youngburg (*35*). For the experiment in Table I, the following buffer was used; 30 mM Tris–HCl (pH 7.5), 3 mM $MgCl_2$, 0.1 mM EDTA, 1 mM EGTA, 1 mM β-mercaptoethanol, 1 μM K23MD or 0.1 μM KIF5AMD and 1 mM ATP. The microtubule concentrations of K23 and KIF5A were 10 μM and 5 μM, respectively.

Tryptophan-mant FRET observation

The spectrum of 2′(3′)-O-(*N*′-methylanthraniloyl)-ATP (mant-ATP) was monitored at excitation and emission wavelengths of 290 and 445 nm, respectively (F-2500 Fluorescence Spectrophotometer; HITACHI). For time-course experiments, 5 μM K23 was added to 1 μM mant-ATP. After the fluorescence intensity of mant-ATP reached a plateau, 1 mM of regular ATP was added. For FRET measurements, the tryptophan was excited at 350 nm. The buffer used for spectral observation was 120 mM NaCl, 30 mM Tris–HCl (pH 7.5) and 3 mM $MgCl_2$.

Fluorescence stopped-flow measurements

Fluorescence stopped-flow measurements were performed with an SX-20 (Applied Photo Physics) stopped-flow apparatus. The dead time of the stopped-flow apparatus was 1.1 ms.

Mant-ATP fluorescence was directly observed with an excitation wavelength of 350 nm, and an excitation wavelength of 290 nm was used for FRET measurements. A 435-nm cut-off filter was used for emission. ATP binding and ADP release were monitored by the changes in the fluorescence of mant-ATP and mant-ADP. Transients shown are the average of 3–5 independent mixings. The transients were best fit to single- or double exponentials, as mentioned in the figure legend. Single exponential data were fit to the equation $y = c + a(\exp(-k_{obs}t))$, and double exponential data were fit to $y = c + a_1(\exp(-k_{obs1}t)) + a_2(\exp(-k_{obs2}t))$, where c is constant and a, a_1 and a_2 are the amplitude coefficients of the reactions with rate constant k_{obs}, $k_{obs\ 1}$ and $k_{obs\ 2}$, respectively.

The observed rates of the exponential phases of mant-ATP binding increased linearly as a function of mant-ATP concentration. These data were fit to Equation 1,

$$k_{obs} = k_1 \cdot k_1^*[ATP] + k_{-1} \quad (1)$$

Table I. Comparison of the ATPase activity of K23MD and mouse kinesin KIF5A.

	Hydrolysis (Pi mol site $mol^{-1}s^{-1}$)		
	Basal	k_{cat}	K_{MT} (μM)
Rice kinesin K23	0.010 ± 0.003	1.3 ± 0.1	1.9 ± 0.8
Mouse kinesin KIF5A	0.03 ± 0.02	58 ± 7	2.0 ± 0.7

Basal: in the absence with microtubule. k_{cat}, V_{max} of ATPase activity. K_{MT} indicates the microtubule concentration at $V_{max}/2$. MT, microtubule. Data given as mean ± SEM of three or four experiments.

where k_{obs} is the observed exponential rate of the fluorescence enhancement, $k_1 \cdot k^*_1$ is the second-order rate constant of ATP binding and k_{-1} is the dissociation rate obtained from the *y*-intercept.

The observed rates of ADP dissociation were hyperbolically dependent on the microtubule concentration. These data were fit to Equation 2,

$$k_{obs} = [Mt] \cdot k_5 / ([Mt] + K_d) + k'_5 \quad (2)$$

where [Mt] is the microtubule concentration, $K_d = k_{-4}/k_4 = [Mt][K \cdot ADP]/[Mt \cdot K \cdot ADP]$, k_5 is the rate of ADP release in the presence of microtubules, and k_5′ is the rate of ADP release in the absence of microtubules and defined by the y-intercept. The nucleotide to protein ratio was held at 5. The buffer conditions were as follows: 20 mM PIPES (pH 6.8), 3 mM $MgCl_2$, 0.1 mM EDTA, 0.1 mM EGTA and 1 mM DTT.

Results

Rice kinesin K23 cloning

K23 is a novel kinesin-like protein found in the rice genome that consists of 945 amino acids and has an *N*-terminal motor domain. Our phylogenetic analysis of K23 using the ClustalW program also confirmed that it is a member of the At1 subfamily of kinesin-7, as described by Guo *et al*. (*5*) (Fig. 1A). All kinesins contain a highly conserved motor domain that has approximately 350 amino acids. To determine the boundaries of the motor domain region, the amino acid sequence of K23 was compared with conventional kinesins whose motor domain regions are known (*36–38*). As shown in Fig. 1B, K23 shares 38.7% amino acid identity with KIF5A and we identified the K23 motor domain (K23MD) as amino acids 36–363. For the comparison of K23 with KIF5A and for convenience, we renumbered leucine 36 as leucine 1, the first methionine from the N terminus as methionine 36 and the last residue of the motor domain, asparagine 363, as 328. K23 lacks the 'loop 5', which is a conserved structure in each kinesin motor domain near the ATPase site.

To biochemically characterize K23, we amplified its motor domain by PCR from cDNA obtained from the NIAS and subcloned this PCR product into an expression vector, pET21a ('Materials and Methods' section). We used the truncated motor domain, because the tail domain of conventional kinesins can inhibit motor activity (*39*).

Expression and preparation of E.coli

The K23 motor domain was expressed in *E. coli* and purified according to the methods described in the 'Materials and Methods' section. Figure 2A shows the elution pattern of His-tagged K23MD from the Co-NTA column. The purity of the K23MD (~36.5 kDa) was confirmed by sodium dodecyl sulphate polyacrylamide gel electrophoresis (SDS–PAGE) (Fig. 2B). The KIF5AMD (~38 kDa) was used as a control and was also purified using the same methods (data not shown).

Characterization of ATPase activity

The biochemical activity of K23 was initially measured using an ATPase activity assay of K23MD. The basal ATPase activity of K23MD was 0.010 ± 0.003 P_i mol site mol^{-1} s^{-1}, which is similar to that of the mouse

Downloaded from http://jb.oxfordjournals.org/ at Changhua Christian Hospital on September 26, 2012

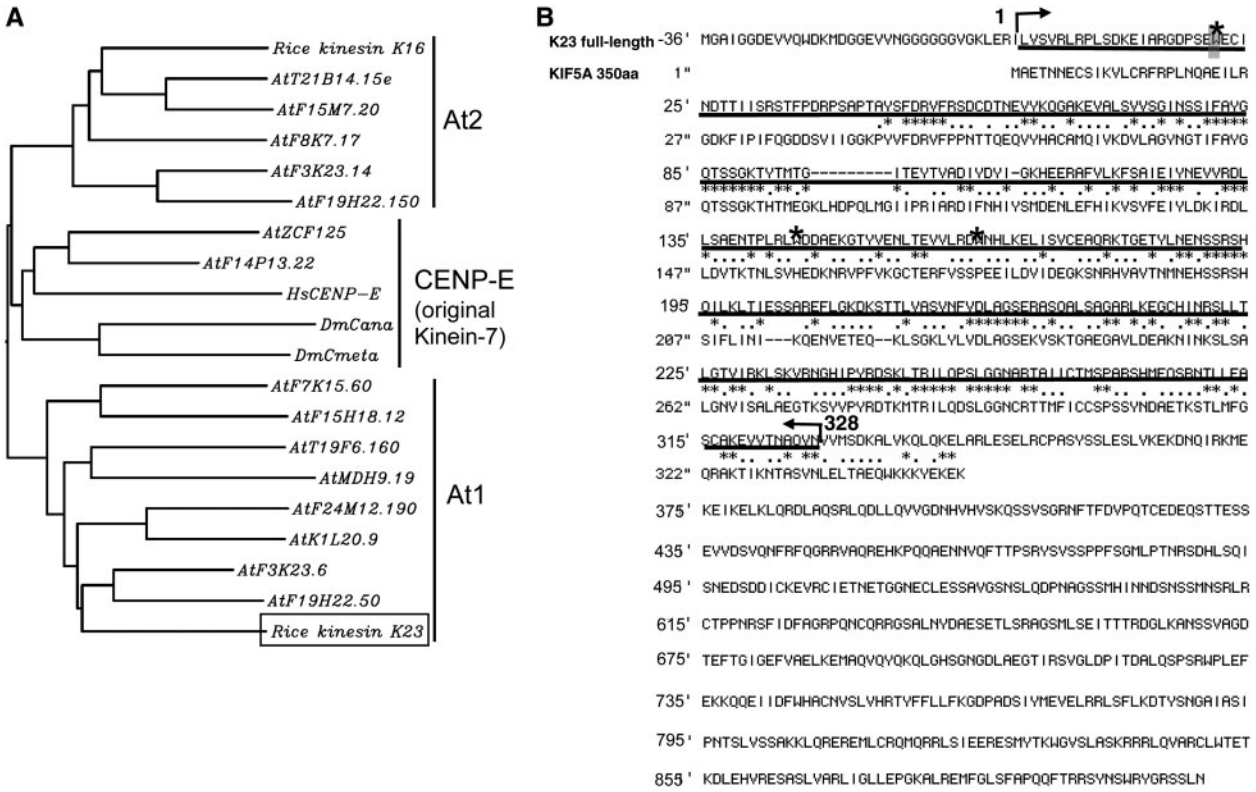

Fig. 1 K23 sequence. (A) Phylogenetic tree of kinesin-7 including the three subfamilies: At1, At2 and CENP-E (original kinesin-7). Phylogenetic analysis of the rice kinesins, other At1 and At2 *Arabidopsis* kinesins and a representative CENP-E (kinesin-7) of the animal kinesins. K23 is boxed (see 'Introduction' section). Phylogenetic analysis was carried out using the full-length amino acid sequences of kinesins using the online software ClustalW version 1.81 (Kyoto University Bioinformatics Center, http://align.genome.jp/). (B) The amino acid sequence of rice kinesin K23. The first methionine and isoleucine 36, which is the first amino acid of the motor domain, were defined as −36 and +1, respectively. The motor domain spans amino acids 1–328. The underlined sequence indicates the motor domain. The motor domain has three tryptophans (asterisks). The tryptophan that is a donor for FRET is shown in a gray box (see 'Text' for the details).

conventional kinesin KIF5AMD (0.03 ± 0.02 P_i mol site $mol^{-1}s^{-1}$). The ATPase activity of K23MD was enhanced ~130-fold by the presence of microtubules. At a saturated microtubule concentration (>10 μM), the steady-state ATPase activity was 1.3 ± 0.1 Pi mol site $mol^{-1}s^{-1}$ with a K_{MT} of 1.9 ± 0.8 μM (Table I and Fig. 3A). This low ATPase activity is consistent with our previous finding that the magnitudes of the enhancement of ATPase activity by microtubules for other plant kinesins are also much lower than that observed for the mouse brain kinesin, KIF5A (57.6 Pi mol site $mol^{-1}s^{-1}$) (*26*, *31*).

We measured the ionic strength dependence of the ATPase activity of K23MD. The ATPase activity of K23MD in the presence of 5 μM microtubules decreased as the concentration of NaCl was increased (Fig. 3B), whereas there was no dependence on the ionic strength in the absence of microtubules. This salt-dependent influence on activity has also been observed for K16 (*26*). The pH dependency of the ATPase activity was also measured for K23. K23 showed optimal activity at pH 7.0 (Fig. 3C), which is the highest among rice kinesins we have previously expressed (*26*, *31*). This may reflect the conformational difference from other kinesins. The optimum pH of rice kinesin K16 and O12 are pH 6.0 and 6.5, respectively (*26*, *31*).

Stability of the ADP-free rice kinesins

The rice kinesin K16, which has a shorter loop 5 than that of KIF5A and is common in the At2 subfamily of kinesin-7, is very stable under ADP-free conditions when incubated at room temperature (*28*). The ATPase activity of K16 following incubation at 24 h and 25°C did not change. The loop 5 of kinesins belonging to the At1 subfamily of kinesin-7 are known to be extremely short or essentially missing. The stability of K23 during ATPase activity was examined to test our hypothesis that its stability is due to the short loop 5 of kinesin-7 (Fig. 4). As shown in Fig. 4, the ATPase activities of ADP-free K23 and K23 with MgADP were reduced by half after 2 and 10 h incubations, respectively, indicating that despite its short loop 5, K23 is not as stable as K16.

Analysis of the fluorescent ATP analogue

In order to analyse the kinetics of K23, we used the following fluorescent ATP analogues: mant-ATP and 2′(3′)-O-[6-(*N*-(7-nitrobenz-2-oxa-1,3-diazol-4-yl)amino) hexanoic]-ATP (NBD-ATP) (*40*). The fluorescence intensities of these ATP analogues vary depending on their hydrophobic or hydrophilic environments. In some cases, we were able to monitor conformational changes of proteins that bind to the fluorescent ATP analogues through changes in the analogues fluorescence intensities.

Downloaded from http://jb.oxfordjournals.org/ at Changhua Christian Hospital on September 26, 2012

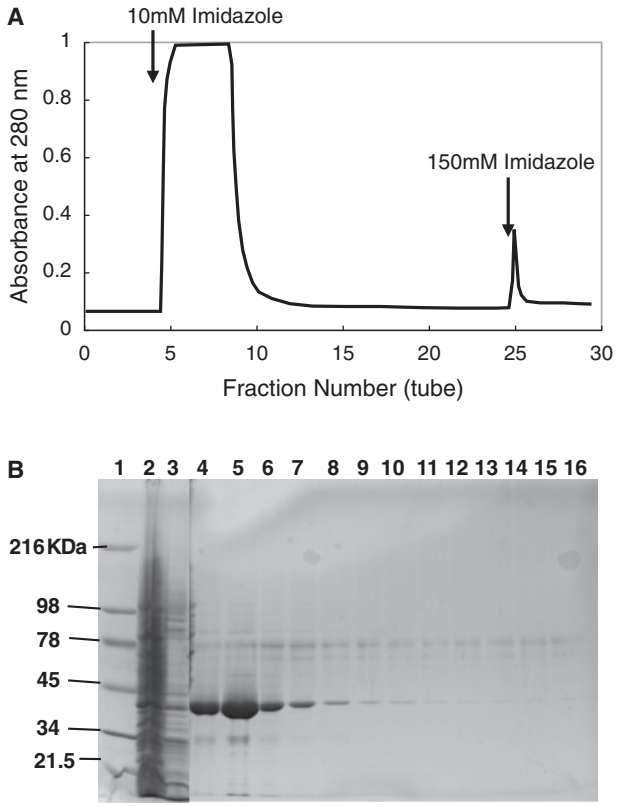

Fig. 2 Affinity purification of kinesin proteins on Co-NTA. (A) An elution diagram of the K23MD purified on Co-NTA. After the sample was loaded, the column was washed with wash buffer at 2.7 ml min^{-1} (300 mM NaCl, 20 mM MOPS-NaOH, pH 7.0, 1 mM $MgCl_2$, 0.1 mM ATP, 0.2 mM β-mercaptoethanol and 10 mM imidazole, pH 7.0) for ~1.5 h. K23MD was then eluted with 150 mM imidazole–HCl (pH 7.5) in wash buffer. (B) Purity was assessed by SDS-gradient gel electrophoresis (7.5–20%). The eluted K23MD was observed as the major band, which is >95% of the total protein in the case of lane 5 on the Coomassie-stained gel. Lane 1, molecular mass markers; Lane 2, the supernatant after centrifugation; Lane 3, lysate precipitant; Lanes 4–16, whole fractions of 150 mM imidazole in wash buffer. Molecular mass markers are 216 kDa, myosin; 98 kDa, phosphorylase b; 78 kDa, BSA; 45 kDa, ovalbumin; 34 kDa, carbonic anhydrase; 21.5 kDa trypsin inhibitor.

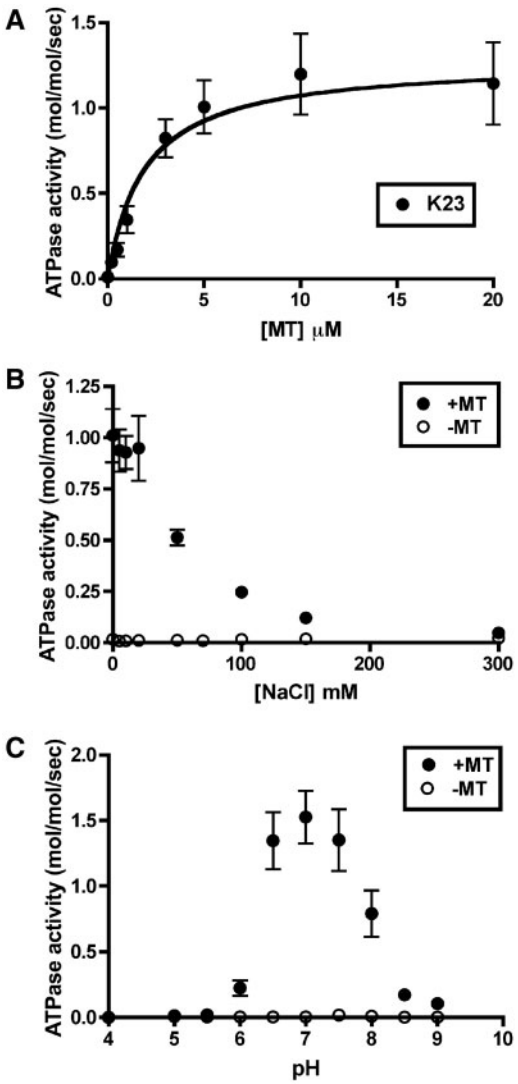

Fig. 3 K23MD ATPase assay. (A) Microtubule concentration dependence of K23MD ATPase activity. ATPase assays were carried out at 25°C in Buffer A (30 mM Tris–HCl, pH 7.5, 3 mM $MgCl_2$, 0.1 mM EDTA, 1 mM EGTA and 1 mM β-mercaptoethanol), 1 μM K23MD and 0–20 μM microtubules. ATPase reactions were started by adding 1 mM ATP. The data were fit to the Michaelis–Menten equation. $V_{max} = 1.3\ s^{-1}$, $K_{MT} = 1.9\ \mu M$. (B) NaCl concentration dependence of the K23MD ATPase activity. ATPase assays were carried out at 25°C in Buffer A. 1 μM K23MD in the absence (open circles) or presence (closed circles) of 5 μM microtubules and various concentrations of NaCl (0–300 mM). The ATPase reactions were initiated by adding 1 mM ATP. (C) pH dependence of K23MD ATPase activity. ATPase assays were carried out at 25°C in Buffer A and 1 μM K23MD in the absence (open circles) or presence (closed circles) of 5 μM microtubules. The ATPase reactions were initiated by adding 1 mM ATP. The following were used as buffers: pH 4.0–5.0, acetate-NaOH; pH 5.5–6.5, MES-NaOH; pH 7.0–7.5, MOPS-NaOH; pH 8.0–9.0, Tris–HCl.

We measured the fluorescence of NBD-ATP on binding to K23MD. However, the fluorescence intensity of NBD-ATP showed little or no change when mixed with K23MD (data not shown). Similarly, negligible changes in the fluorescence-intensity of mant-ATP (excitation and emission wavelengths were 350 and 445 nm, respectively) were observed when mixed with K23MD (Fig. 5A). Furthermore, at the highest concentration of mant-ATP, the changes in the fluorescence-intensity were significantly reduced and too small to use for a kinetic study.

Analysis of the interaction of mant-ATP with tryptophan in FRET experiments

We expected that tryptophan, whose excitation and emission wavelengths are 290 and 350 nm, respectively, could be a FRET-donor, and mant-ATP, whose excitation and emission wavelengths are 350 and 445 nm, respectively, could be a FRET-acceptor. We initially confirmed that there were no emissions for mant-ATP at an excitation wavelength of 290 nm (data not shown). The fluorescence spectra of the K23MD wild-type (WT) at an excitation wavelength of 290 nm with (solid line) or without (broken line) mant-ATP were monitored (Fig. 5B). It is worth noting that the emission of K23MD WT in the presence of mant-ATP at 445 nm was much more intense than that of K23MD WT alone. This emission at 445 nm is most likely caused by the FRET between mant-ATP and the tryptophan in K23MD WT.

Downloaded from http://jb.oxfordjournals.org/ at Changhua Christian Hospital on September 26, 2012

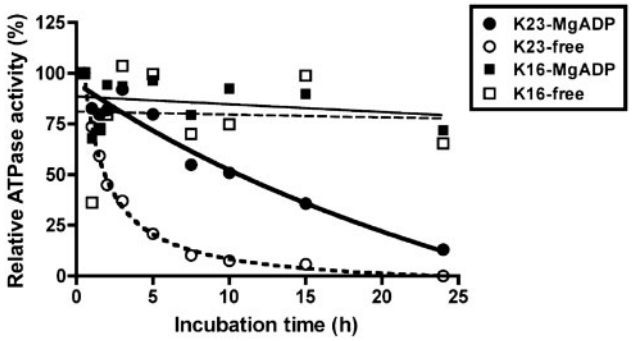

Fig. 4 The stability of the ADP-free rice kinesins. ADP-free kinesin MDs (K23: open circles, K16: open squares) and ADP-bound kinesin MDs (K23: closed circles, K16: closed squares) were incubated in 120 mM NaCl, 30 mM Tris–HCl (pH 7.5), 1 mM $MgCl_2$, 1 mM DTT and 0.1 mM ATP for 0.5–24 h at 25°C. After incubation, ATPase assays were carried out at 25°C in Buffer A, 1 μM kinesin MD and 5 μM microtubules. ATPase reactions were initiated by adding 1 mM ATP.

The mant-ATP binding and release of K23MD was observed by monitoring the FRET-mediated emission of mant-ATP at 445 nm and at an excitation wavelength of 290 nm for tryptophan (Fig. 5C). K23MD was added to mant-ATP at a molar concentration ratio of 5 : 1. The fluorescence intensity increased when mant-ATP was injected and bound to the ATP-binding site of K23. The fluorescence reached a plateau at ~100 s and the addition of 1 mM ATP caused a sharp decrease in the fluorescence, reflecting a release of mant-ATP from the K23 ATP-binding site. Approximately 10% of mant-ATP fluorescence still remained even following the addition of 1,000-fold ATP (Figs 5C and 6B), indicating that mant-ATP was not fully released from K23. This may be due to the non-specific binding of mant-ATP to K23. We have previously observed non-specific binding of a photo-affinity labeled ATP analogue, mant-8-azido-ATP, to skeletal muscle myosin (*41*).

K23MD has three tryptophans: W21, W145 and W165 (Fig. 1). W21 is considered to be close enough to the ATP-binding site of K23MD WT to monitor the FRET between W21 and mant-ATP (Fig. 6A and B). Since K23MD WT has three tryptophans, we constructed a double mutant of K23MD W145F/W165F, to confirm that W21 is the primary donor in the FRET measurement. As shown in Figs 5B and 6A, the intensities of the presumed FRET-mediated fluorescence from mant-ATP at 445 nm were similar to those observed in K23MD WT in the presence or absence of mant-ATP. These results suggest that the W21 in K23MD WT acts as the dominant donor residue in the FRET measurements.

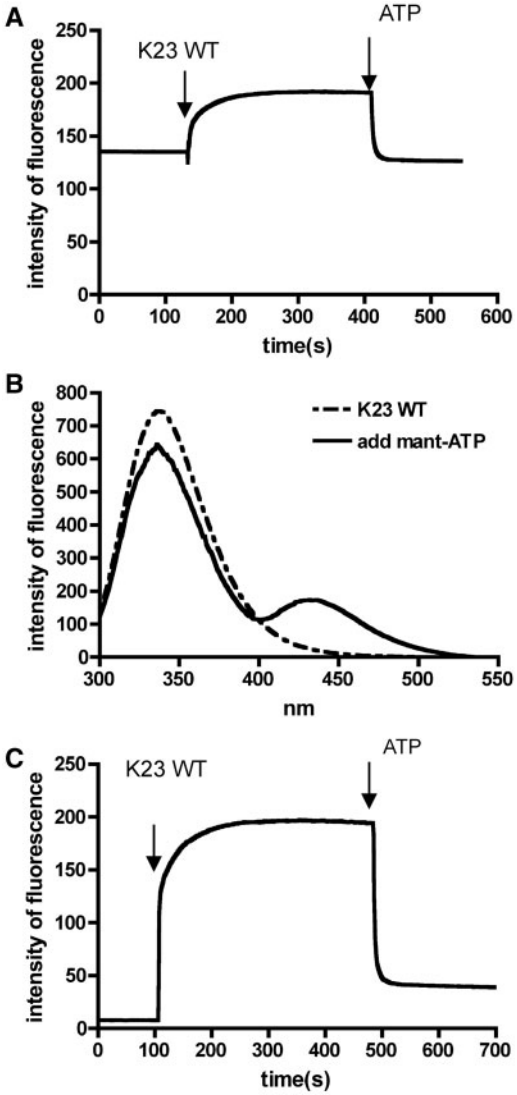

Fig. 5 The fluorescence time course and spectrum of K23MD WT. (A) The time course of mant-ATP binding to and release from K23MD. The fluorescence intensity of 1 μM mant-ATP increased slightly following the addition of K23MD WT (final concentration, 5 μM) and decreased with the addition of regular-ATP (final concentration, 1 mM). The excitation and emission wavelengths were 350 and 445 nm, respectively. (B) The interaction of K23MD WT with mant-ATP in the fluorescence experiments. The representative FRET experiments with an excitation wavelength of $\lambda_{ex} = 290$ nm are shown. The dotted and bold lines indicate 5 μM K23MD in buffer without and with a final concentration of 1 μM mant-AT, respectively. (C) FRET analysis of mant-ATP binding to and release from K23MD. The fluorescence intensity at 1 μM mant-ATP increased following the addition of K23MD WT (final concentration, 5 μM) and decreased after adding ATP (final concentration 1 mM). The excitation and emission wavelengths were 290 and 445 nm, respectively. The experiments were conducted under the following conditions: 120 mM NaCl, 30 mM Tris–HCl, pH 7.5 and 3 mM $MgCl_2$ at 25°C.

Kinetic analysis of K23 using FRET between a tryptophan and mant-ATP

ATP hydrolysis is proposed to be a cross-bridge cycle as shown in Scheme 1: two step ATP binding ($k_1 \cdot k^*_1$), ATP hydrolysis (k_2), Pi release (k_3), ADP release (k_5) and microtubule association (k_4). We determined the ATP binding and ADP release steps of the ATPase cycle. The rate of ATP binding to K23 was measured by monitoring the changes of mant fluorescence (Fig. 7A and B), according to the following mechanism:

$$\mathrm{K} + \mathrm{ATP} \underset{}{\overset{k'_1}{\rightleftarrows}} \mathrm{K(ATP)} \overset{k^{*\prime}{}_1}{\rightarrow} \mathrm{K \cdot ATP}$$

The reaction is modelled as a two-step reaction: formation of the collision complex [K(ATP)] followed by

Downloaded from http://jb.oxfordjournals.org/ at Changhua Christian Hospital on September 26, 2012

a conformational change with high-fluorescence. The nucleotide to protein ratio was held at 5. This is a compromise between achieving strictly first-order kinetics and maintaining a measurable fluorescence change relative to the background signal. The binding of mant-ATP resulted in an increase in the fluorescence intensity (Fig. 7A). The data were fit to a double exponential curve. The observed rates of the exponential phase increased linearly as a function of mant-ATP concentration (Fig. 7B). The fast phase reflected the binding of mant-ATP to the catalytic site. Since the other phase was extremely slow, the phase may not be related to the ATPase cycle. This phase may be induced by non-specific binding of mant-ATP to K23. According to Equation 1, the rate constant for ATP binding to K23 ($k_1' \cdot k^*_1'$) is determined from the initial slope, and was $3.2\,\mu M^{-1}\cdot s^{-1}$ in the absence of microtubules. The ATP dissociation rate was determined from the y-intercept as $5\,s^{-1}$. As shown in Table II, the rate constant for ATP binding to K23 in the presence of microtubules is $5\,\mu M^{-1}\cdot s^{-1}$. Based on these parameters, the rate of ATP binding under physiological ATP conditions (~2 mM ATP) is $>6000\,s^{-1}$ if the rate constant linearly increases as the ATP concentration increases. This is 5000-fold faster than the cycle rate.

We next examined the rate of mant-ADP release from K23. The rate of ADP dissociation from K23 was measured by monitoring the rate of decrease of the mant-fluorescence upon binding microtubules, according to following mechanism:

$$k_4 \rightarrow k_5$$
$$K \bullet ADP + Mt \rightleftharpoons Mt \bullet K \bullet ADP \rightleftharpoons Mt \bullet K + ADP$$

K23 was first incubated with an equimolar amount of mant-ADP. Mant-ADP was rapidly mixed with various concentrations of microtubules and 1 mM ATP. The presence of excess amounts of ATP prevented mant-ADP from rebinding to K23. A representative transient is shown in Fig. 7C. The transient was fit to a double exponential. The fast phase of the dissociation rate was $2.91\,s^{-1}$ and the slow phase was $0.32\,s^{-1}$. This slow rate is approximately 20-times slower than the cycle rate and cannot account for the steady-state ATPase cycle. At present, we do not understand the origin of this slow change in the fluorescence intensity. The observed rates were plotted as a function of microtubule concentrations (Fig. 7D). According to Equation 2, the ADP dissociation rate in the presence (k_5) and absence (k_5') of microtubules was determined to be $2.8\,s^{-1}$ and $0.67\,s^{-1}$, respectively. The ADP off rate ($2.8\,s^{-1}$) was twice as fast as the k_{cat}, suggesting that the ADP dissociation step would contribute to the overall ATPase rate. These results suggest that the kinetic mechanism of K23 is different from mammalian kinesins (*29*, *30*, *33*, *42–46*). The half-maximum microtubule concentration is 0.7 μM, which is similar to the K_{MT} of the steady-state ATPase activity.

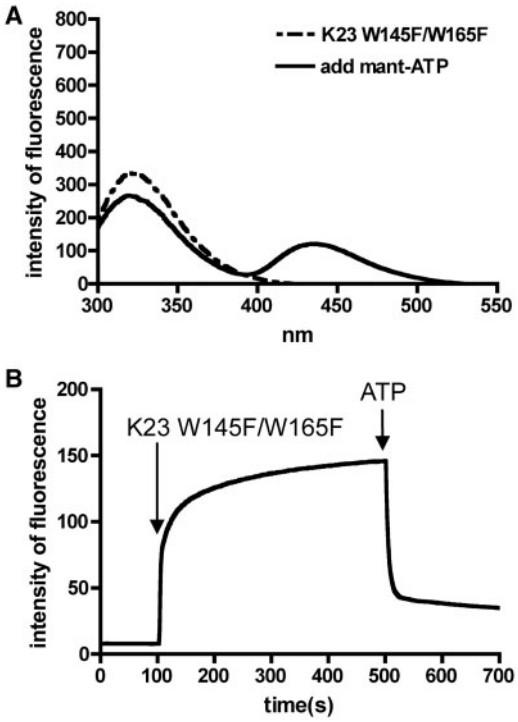

Fig. 6 The fluorescence spectra of K23MD W145F/W165F. (A) The interaction of K23MD W145F/W165F with mant-ATP in fluorescence experiments. A representative FRET experiment with an excitation wavelength of $\lambda_{ex} = 290$ nm is shown. The dotted and bold lines indicate 5 μM K23MD W145F/W165F in buffer without and with a 1 μM final concentration of mant-ATP. (B) FRET analysis of mant-ATP binding to and release from K23MD W145F/W165F. The fluorescence intensity of 1 μM mant-ATP increased following the addition of K23MD WT W145F/W165F (final concentration, 5 μM) and decreased after adding ATP (final concentration, 1 mM). The excitation and emission wavelengths were 290 and 445 nm, respectively. The experiments were conducted under the following conditions: 120 mM NaCl, 30 mM Tris–HCl, pH 7.5 and 3 mM $MgCl_2$ at 25°C.

Kinetic analysis of the KIF5A L25W mutant using Trp-mant FRET

To test the validity of the kinetic characteristics of K23 using FRET, we selected a mouse conventional kinesin, KIF5A, which has been extensively characterized, and introduced a tryptophan residue as a FRET-donor. A point mutation, L25W, was introduced in

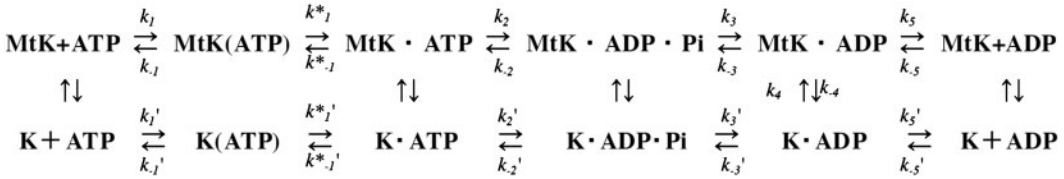

Scheme 1 ATPase cycle of Kinesin. K, K23; Mt, microtubule; k, in the presence of microtubules; k′, in the absence of microtubules.

Downloaded from http://jb.oxfordjournals.org/ at Changhua Christian Hospital on September 26, 2012

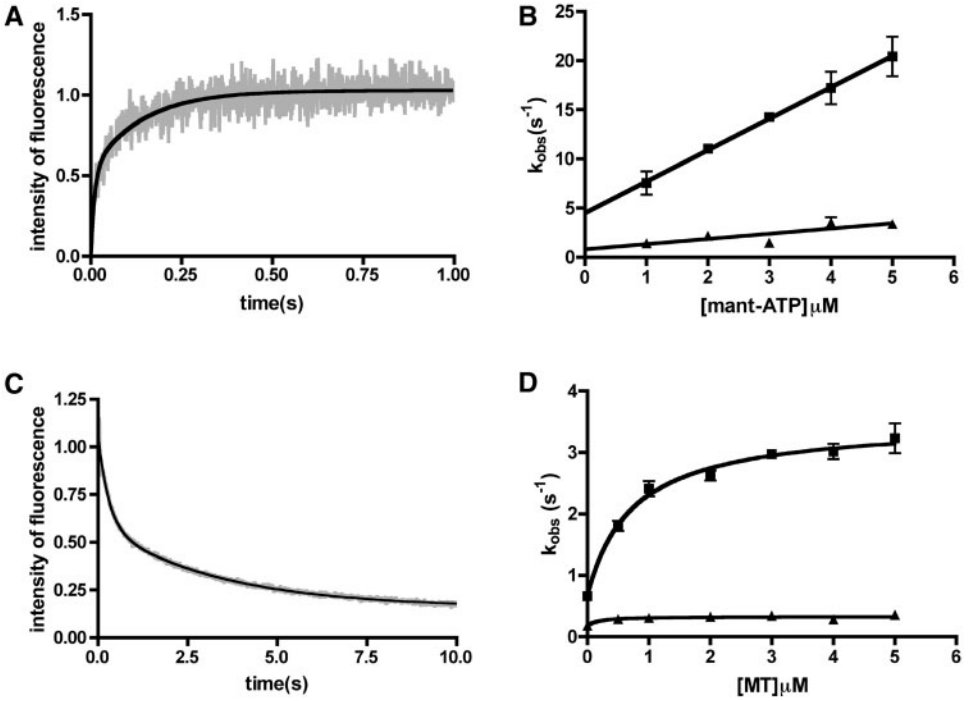

Fig. 7 Kinetic analysis of K23MDWT using Trp-mant FRET. (A) ATP binding to K23MD WT in the absence of microtubules measured by Trp-mant FRET. A representative fluorescence transient is shown. The fluorescence enhancement was observed upon the addition of 5 μM mant-ATP to 1 μM K23MD WT in the stopped-flow apparatus. The reaction was monitored with respect to mant fluorescence intensity using the Trp-mant FRET technique. Smooth black lines show the fit to a double exponential curve. The rate constants were 22.2 s^{-1} and 3.48 s^{-1}. (B) The observed rate constants were plotted as a function of mant-ATP concentration (1–5 μM). Both fast and slow phases were observed to increase linearly as the concentration of mant-ATP was increased. For K23MD WT, the data yielded a second order rate constant for mant-ATP binding in the absence of microtubules of 3.2 $\mu M^{-1}\cdot s^{-1}$ for the fast phase and 0.53 $\mu M^{-1}\cdot s^{-1}$ for the slow phase. (C) A representative transient of ADP release in the presence of microtubules. The fluorescence transient was observed upon the addition of 5 μM microtubules and 1 mM ATP to 2 μM mantADP•K23MD in the stopped-flow apparatus Smooth black lines show the fit to the double exponential curve. The rate constants were 2.91 s^{-1} and 0.32 s^{-1}. The buffer conditions were the same as those described in (A). (D) The ADP release rate. The observed rates were plotted as a function of the microtubule concentrations. These data were fit to Eq 2. $k_5 = 2.8\ s^{-1}$, $k_{-5} = 0.67\ s^{-1}$.

Table II. Experimentally determined rate constants for K23 and a conventional kinesin.

	K23	Conventional
Steady-state ATPase		
−MT		
k_{cat} (s^{-1})	0.010 ± 0.003	0.02[a]
+MT		
k_{cat} (s^{-1})	1.3 ± 0.1	89[b]
K_{MT} (μM)	1.9 ± 0.8	2.0 ± 0.7
ATP binding		
−MT		
k_{on} ($\mu M^{-1}s^{-1}$) $\boldsymbol{k_1'\cdot k^*_1'}$	3.2 ± 0.4	9[a]
k_{off} (s^{-1})	5 ± 1	–
K_d (= k_{off}/k_{on}) (μM)	1.6	–
+MT		
k_{on} ($\mu M^{-1}s^{-1}$) $k_1\cdot k^*_1$	5 ± 1	20[b]
k_{off} (s^{-1})	7 ± 3	113[b]
K_d (= k_{off}/k_{on})(μM)	1.4	23[b]
ADP release		
−MT		
k_{off} (s^{-1}) k_5'	0.67 ± 0.02	0.02[a]
+MT		
k_{off} (s^{-1}) k_5	2.8 ± 0.2	303[b]

Data given as mean ± SEM of three or four experiments.
[a]Ma Y.Z. and Taylor E.W., 1997 (*44*).
[b]Moyer M.L. *et al.*, 1998 (*43*).
MT, microtubule; –, no data.

Downloaded from http://jb.oxfordjournals.org/ at Changhua Christian Hospital on September 26, 2012

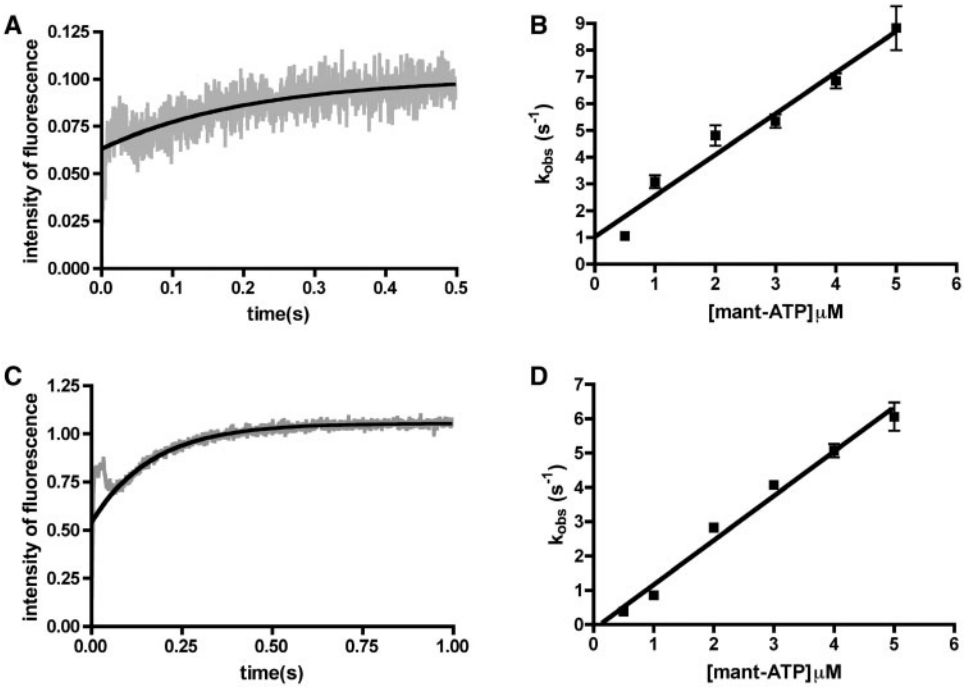

Fig. 8 Kinetic analyses for KIF5A WT and the L25W mutant. (A) ATP binding to KIF5AMD WT in the presence of microtubules. Fluorescence transients were observed upon the addition of 5 μM mant-ATP to KIF5A WT (final concentration, 1 μM) in the presence of microtubules (final concentration, 1.25 μM). Smooth black lines show the fit of the single exponential curve. The rate constant was 6.67 s^{-1}. The buffer conditions were as follows: 20 mM PIPES–NaOH, pH 6.8, 3 mM $MgCl_2$, 0.1 mM EDTA, 0.1 mM EGTA, 1 mM DTT and 10 μM taxol at 25°C. The reaction was monitored by measuring the mant fluorescence intensity. (B) The observed rates of the transients were plotted as a function of the mant-ATP concentration (0.5–5 μM). For the KIF5A WT, the data provided a second-order rate constant for mant-ATP binding in the presence of microtubules of 1.54 $\mu M^{-1} \cdot s^{-1}$. (C) ATP binding to KIF5AMD L25W in the presence of microtubules measured by Trp-mant FRET. The fluorescence transients of KIF5A L25W were measured in a similar manner to those of WT in (A). Smooth black lines show the fit of the single exponential curve. The rate constant was 5.98 s^{-1}. The reaction was monitored by measuring the mant fluorescence intensity using the Trp-mant FRET technique. (D) The observed rate constants were plotted as a function of the mant-ATP concentration (0.5–5 μM). For the KIF5A L25W mutant, the data provided a second order rate constant for mant-ATP binding in the presence of microtubules of 1.30 $\mu M^{-1} \cdot s^{-1}$.

KIF5AMD, which was intended to be the corresponding position of the W21 of K23. This mutation was also close enough to mant-ATP to allow FRET between the donor and acceptor probes. KIF5AMD WT was used as a control. The KIF5AMD L25W and WT were measured using the same stopped-flow method used for the K23MD WT described above. Fig. 8A and C show the transients of mant-ATP binding to KIF5AMD WT and KIF5AMD L25W in the presence of microtubules. The second-order rate constants of ATP binding to KIF5A WT and L25W were 1.54 (Fig. 8B) and 1.30 $M^{-1} \cdot s^{-1}$ (Fig. 8D), respectively. These results suggest that the FRET from the tryptophan at the corresponding position of W21 in K23 to the mant-ATP at the K23 ATP-binding site is generally observable in kinesins, and therefore the donor and acceptor moieties are proximal to each other.

Discussion

Recently, the complete genomic sequences of *Arabidopsis* and rice revealed the existence of plant-specific kinesin subfamilies. Moreover, the number of members to these subfamilies was considerable and included the At1 and At2 subfamilies of kinesin-7 and a subgroup of kinesin-14 (*5*, *14*, *18*). Plant-specific kinesins are expected to play plant-specific roles. CENP-E, which is an animal kinesin that previously represented kinesin-7, is a plus-end microtubule motor that plays a role in chromosome congregation to the plate during prometaphase (*19*). Some kinesins of At1 or At2 regulate the localization of the phragmoplast and are involved in its construction (*7*, *20*). We cloned and characterized a novel rice kinesin, K23, which belongs to the plant-specific At1 subfamily (Fig. 1A).

K23MD shares 38.7 and 43.9% amino acid identity with mouse conventional kinesin KIF5AMD (Fig. 1B) and rice kinesin K16 (data not shown), respectively. Unlike other known kinesins, K23 has only one amino acid sequence at the corresponding position to loop 5. Most of the members of At1 have no loop 5. The rice kinesin K16 has a short loop 5 composed of only seven residues; this appears to be a hallmark of the At2 and CENP-E subfamilies. Loop 5 has been reported to be important in the biochemical functions and/or regulation of kinesins (*27*, *47*, *48*). The unique enzymatic properties of K23 may be related to the absence of loop 5, and this absence probably reflects plant specific physiological roles.

We have been focusing on loop 5 to verify the relation between this loop and the function of kinesins. Loop 5 appears to be an important region in the motor domain of kinesin and controls enzymatic characteristics (*49*). Rice kinesin K16 belonging to At2 has

Downloaded from http://jb.oxfordjournals.org/ at Changhua Christian Hospital on September 26, 2012

a shorter loop 5 than found in a conventional kinesin, and has unique enzymatic properties. The purification of K16 in the absence MgADP has been achieved and this protein is very stable (*26*–*28*). Recently, our crystallographic study of K16 revealed that the unique conformations of the functional key regions, *e.g.* the short loop 5 and the Mg-stabilizing residues, are located further from the Mg ion than observed in other kinesins (*28*). Interestingly, our recent experiments showed that the truncated or elongated loop 5 of K16 strongly trapped Mg-ATP in the active site and abolished ATPase activity (*28*). Therefore, this observation suggests that the length and/or conformation of loop 5 affects the conformation of the catalytic site, which may be related to the stability of the protein. As shown in Fig. 4, the ATPase activity of K16 under nucleotide-free conditions is as stable as that in the presence of Mg-ADP for 24 h, whereas the ATPase activity of nucleotide-free K23 decreased quickly in just a few hours. This difference in stability might be reflected by the difference in the conformations of the functional key regions, including loop 5.

In the absence of microtubules, the basal steady-state ATPase activity of K23MD was similar to that of the mouse conventional kinesin KIF5AMD. Conversely, in the presence of microtubules, K23MD showed lower ATPase activity than KIF5AMD (Fig. 3 and Table I) with high affinity for microtubules. The difference in the ATPase activities between K23 and KIF5A may be due to the difference in the amino acid sequences of plant and animal tubulins (*50*, *51*). Interestingly, the ATPase properties of K23MD were similar to that of CENP-E, which belongs to the kinesin-7 subfamily recently reported by Gilbert *et al.* (*52*). CENP-E is known to have critical roles in mitosis, including the establishment of microtubule (MT)-chromosome linkage and the movement of mono-oriented chromosomes on kinetochore-microtubules for proper alignment at metaphase (*52*). Therefore, K23 may be related to similar physiological roles.

Greater ionic strength results in lower ATPase activity, suggesting that the interaction of K23MD with microtubules depends primarily on electrostatic interactions, which is consistent with the results of other rice kinesins, O12 and K16 (*26*, *31*). The optimum pH values of K16 and K23 are 6.0 and 7.0, respectively; the optimum pH of K23 is slightly higher than other known plant kinesins, which have optimum pH values between 6.0 and 6.5. The different optimum pH of K23 indicates that its subcellular localization is different from other kinesins (*26*, *31*).

For the biochemical analysis of K23, we attempted to directly measure fluorescent ATP analogues, NBD-ATP and mant-ATP, during their binding to K23MD. However, negligible or no change in their fluorescence intensities was observed. While modeling the structure of K23 to that of K16 (*28*), one of the three tryptophan residues in K23, W21, appeared to be proximal to the ATP-binding site, allowing FRET measurements with an ATP analogue. In contrast, W145 and W165 were located distal from the ATP-binding site. While exploiting W21 of K23 as a FRET donor to an acceptor (mant-ATP), we were able to monitor conformational changes to K23 during the ATPase cycle. Since the fluorescence of mant-ATP upon binding to K23 was not changed by excitation at 350 nm, the observed enhancement of mant fluorescence at 290 nm excitation must reflect FRET between mant-ATP and W21. To confirm that W21 actually operates as a FRET donor, we constructed a double mutant, K23MD W145F/W165F, which has only W21. The FRET efficiency ($E = 0.22$) of K23MD W145F/W165F was slightly greater than that ($E = 0.17$) of K23MD WT (Figs 6A and 5B), indicating that W21 is the predominant FRET donor. Previously, a similar kinetic study on wild-type Eg5 utilizing the FRET between an intrinsic tryptophan and mant-ADP was reported by Maliga *et al.* (*48*). The FRET donor on the Eg5 is likely to be W127, an amino acid located in loop 5 of the Eg5 motor domain and close to the nucleotide binding pocket of Eg5 (*48*).

K23MD WT was analysed by Trp-mant FRET using stopped-flow measurements. The second-order rate constant of ATP binding to K23MD was $3.2\,M^{-1}{\cdot}s^{-1}$ in the absence of microtubules. This result is similar to that of conventional kinesins. The comparison of the steady state ATPase and kinetic rates of K23 and a conventional kinesin is presented in Table II. One of the major differences between K23 and a conventional kinesin is the dissociation constant of ATP. The ATP dissociation constant of a conventional kinesin is 23 μM in the presence of a microtubule. This is mainly due to the faster dissociation rate of ATP ($113\,s^{-1}$). With respect to K23, the ATP dissociation constant does not change in the absence or presence of microtubules with values of 1.6 μM and 1.4 μM, respectively. This suggests that the conformation of microtubule-bound K23 is different compared with a conventional kinesin.

The rate of mant-ADP release from K23 was $2.8\,s^{-1}$ in the presence of microtubules, which is lower when compared with KIF5A ($303\,s^{-1}$). The ADP off-rate from microtubule-bound K23 is two times faster than the steady state ATPase activity ($1.3\,s^{-1}$), suggesting that the ADP dissociation step would contribute to the overall ATPase rate and such an observation is not found in conventional kinesins. Consequently, K23 exhibits unique kinetic characteristics.

To confirm if our biochemical analyses of K23 by FRET are valid, we used a mouse conventional kinesin, KIF5A, which has been well characterized. The KIF5AMD does not have an intrinsic tryptophan to act as a donor of FRET near the ATPase site. Leucine 25 in KIF5AMD, which corresponds to position W21 of K23, was mutated to a tryptophan. The kinetic parameters of the ATPase cycle of KIF5AMD L25W were determined using FRET by stopped-flow measurements. The ATP-binding rate constant of KIF5A L25W by Trp-mant FRET in the presence of microtubules was similar to that of KIF5A WT (Fig. 8D), indicating that this mutation does not affect the biochemical properties of KIF5A WT. Furthermore, KIF5A L25W also exhibited similar ATPase activity to KIF5A WT ($43.3\,Pi\,mol\ site\ mol^{-1}s^{-1}$). Consequently, our results of kinetic parameters for

Downloaded from http://jb.oxfordjournals.org/ at Changhua Christian Hospital on September 26, 2012

K23 obtained using FRET are thought to be appropriate values. Crystal structure analysis will provide further insight into the specific biochemical activity of K23.

In conclusion, the characterization of the plant-specific rice kinesin K23 was carried out. The ATPase activity of K23 was lower than conventional kinesins, but the same as other rice kinesins. The affinity of K23 to microtubules was very high. The rate of ATP binding to K23MD was not accelerated by microtubules. The ADP-release rate of K23MD in the presence of microtubules was lower than K16 and KIF5A. In addition, the introduction of a tryptophan residue at the corresponding W21 position of K23 in other kinesins, in conjunction with FRET and fluorescent ATP analogues, may represent a simple direct way to monitor the hydrolysis of ATP using a Trp-mant FRET approach.

Acknowledgements

We thank Dr Taketoshi Kambara (Department of Physics, School of Science, The University of Tokyo) for intellectual discussions and helpful comments during this study.

Funding

Grant-in-Aid for Scientific Research C (*19570047*) from the Ministry of Education, Culture, Sports, Science and Technology of Japan.

Conflict of interest

None declared.

References

1. Hirokawa, N. and Noda, Y. (2008) Intracellular transport and kinesin superfamily proteins, KIFs: structure, function, and dynamics. *Physiol. Rev.* **88**, 1089–1118
2. Hirokawa, N., Noda, Y., Tanaka, Y., and Niwa, S. (2009) Kinesin superfamily motor proteins and intracellular transport. *Nat. Rev. Mol. Cell. Biol.* **10**, 682–696
3. Miki, H., Okada, Y., and Hirokawa, N. (2005) Analysis of the kinesin superfamily: insights into structure and function. *Trends Cell Biol.* **15**, 467–476
4. Vale, R.D. (2003) The molecular motor toolbox for intracellular transport. *Cell* **112**, 467–480
5. Guo, L., Ho, C.M., Kong, Z., Lee, Y.R., Qian, Q., and Liu, B. (2009) Evaluating the microtubule cytoskeleton and its interacting proteins in monocots by mining the rice genome. *Ann. Bot.* **103**, 387–402
6. Hiwatashi, Y., Obara, M., Sato, Y., Fujita, T., Murata, T., and Hasebe, M. (2008) Kinesins are indispensable for interdigitation of phragmoplast microtubules in the moss Physcomitrella patens. *Plant Cell* **20**, 3094–3106
7. Sazuka, T., Aichi, I., Kawai, T., Matsuo, N., Kitano, H., and Matsuoka, M. (2005) The rice mutant dwarf bamboo shoot 1: a leaky mutant of the NACK-type kinesin-like gene can initiate organ primordia but not organ development. *Plant Cell Physiol.* **46**, 1934–1943
8. Lu, L., Lee, Y.R., Pan, R., Maloof, J.N., and Liu, B. (2005) An internal motor kinesin is associated with the Golgi apparatus and plays a role in trichome morphogenesis in Arabidopsis. *Mol. Biol. Cell* **16**, 811–823
9. Preuss, M.L., Kovar, D.R., Lee, Y.R., Staiger, C.J., Delmer, D.P., and Liu, B. (2004) A plant-specific kinesin binds to actin microfilaments and interacts with cortical microtubules in cotton fibers. *Plant Physiol.* **136**, 3945–3955
10. Tamura, K., Nakatani, K., Mitsui, H., Ohashi, Y., and Takahashi, H. (1999) Characterization of katD, a kinesin-like protein gene specifically expressed in floral tissues of Arabidopsis thaliana. *Gene* **230**, 23–32
11. Dymek, E.E., Goduti, D., Kramer, T., and Smith, E.F. (2006) A kinesin-like calmodulin-binding protein in Chlamydomonas: evidence for a role in cell division and flagellar functions. *J. Cell Sci.* **119**, 3107–3116
12. Asada, T., Kuriyama, R., and Shibaoka, H. (1997) TKRP125, a kinesin-related protein involved in the centrosome-independent organization of the cytokinetic apparatus in tobacco BY-2 cells. *J. Cell Sci.* **110**, 179–189
13. Ambrose, J.C. and Cyr, R. (2008) Mitotic spindle organization by the preprophase band. *Mol. Plant.* **1**, 950–960
14. Preuss, M.L., Delmer, D.P., and Liu, B. (2003) The cotton kinesin-like calmodulin-binding protein associates with cortical microtubules in cotton fibers. *Plant Physiol.* **132**, 154–160
15. Hamada, T. (2007) Microtubule-associated proteins in higher plants. *J. Plant Res.* **120**, 79–98
16. Reddy, A.S. and Day, I.S. (2001) Kinesins in the Arabidopsis genome: a comparative analysis among eukaryotes. *BMC Genomics* **2**, 2
17. Richardson, D.N., Simmons, M.P., and Reddy, A.S. (2006) Comprehensive comparative analysis of kinesins in photosynthetic eukaryotes. *BMC Genomics* **7**, 18
18. Dagenbach, E.M. and Endow, S.A. (2004) A new kinesin tree. *J. Cell Sci.* **117**, 3–7
19. Yen, T.J., Li, G., Schaar, B.T., Szilak, I., and Cleveland, D.W. (1992) CENP-E is a putative kinetochore motor that accumulates just before mitosis. *Nature* **359**, 536–539
20. Takahashi, Y., Soyano, T., Sasabe, M., and Machida, Y. (2004) A MAP kinase cascade that controls plant cytokinesis. *J. Biochem.* **136**, 127–132
21. Staehelin, L.A. and Hepler, P.K. (1996) Cytokinesis in higher plants. *Cell* **84**, 821–824
22. Jürgens, G. (2005) Plant cytokinesis: fission by fusion. *Trends Cell Biol.* **15**, 277–283
23. Nishihama, R., Soyano, T., Ishikawa, M., Araki, S., Tanaka, H., Asada, T., Irie, K., Ito, M., Terada, M., Banno, H., Yamazaki, Y., and Machida, Y. (2002) Expansion of the cell plate in plant cytokinesis requires a kinesin-like protein/MAPKKK complex. *Cell* **109**, 87–99
24. Sasabe, M. and Machida, Y. (2006) MAP65: a bridge linking a MAP kinase to microtubule turnover. *Curr. Opin. Plant Biol.* **9**, 563–570
25. Strompen, G., El Kasmi, F., Richter, S., Lukawitz, W., Assaad, F. F., Jurgens, G., and Mayer, U. (2002) The Arabidopsis HINKEL gene encodes a kinesin-related protein involved in cytokinesis and is expressed in a cell cycle-dependent manner. *Curr. Biol.* **12**, 153–158
26. Umeki, N., Mitsui, T., Umezu, N., Kondo, K., and Maruta, S. (2006) Preparation and characterization of a novel rice plant-specific kinesin. *J. Biochem.* **139**, 645–654
27. Umeki, N., Mitsui, T., Kondo, K., and Maruta, S. (2006) Conformational change of the loop L5 in rice kinesin motor domain induced by nucleotide binding. *J. Biochem.* **139**, 857–864
28. Tanaka, K., Umeki, N., Toshiaki, M., Fujimoto, Z., and Maruta, S. (2010) Crystallographic analysis reveals a unique conformation of the ADP-bound novel rice kinesin K16. *Biochem. Biophys. Res. Commun.* **401**, 251–256
29. Ma, Y.-Z and Taylor, E.W. (1995) Kinetic Mechanism of Kinesin Motor Domain. *J. Biochem.* **34**, 13233–13241

Downloaded from http://jb.oxfordjournals.org/ at Changhua Christian Hospital on September 26, 2012

30. Huang, T.G. and Hackney, D.D. (1994) Drosophila kinesin minimal motor domain expressed in Escherichia coli. Purification and kinetic characterization. *J. Biol. Chem.* **269**, 16493–16501
31. Umezu, N., Umeki, N., Mitsui, T., Kondo, K., and Maruta, S. (2011) Characterization of a novel rice kinesin O12 with a calponin homology domain. *J. Biochem.* **149**, 91–101
32. Williams, R.C. Jr and Lee, J.C. (1982) Preparation of tubulin from brain. *Methods Enzymol.* **85**, 376–385
33. Hackney, D.D. (1988) Kinesin ATPase: rate-limiting ADP release. *Proc. Natl. Acad. Sci. USA* **85**, 6314–6318
34. Itzhaki, R.F. and Gill, D.M. (1964) A micro-biuret methods for estimating protein. *Anal. Biochem.* **121**, 401–410
35. Youngburg, G.E. and Youngburg, M.V. (1930) A system of blood phosphorus analysis. *J. Lab. Clin. Med.* **16**, 158–166
36. Kozielski, F., Sack, S., Marx, A., Thormählen, M., Schönbrunn, E., Biou, V., Thompson, A., Mandelkow, E.M., and Mandelkow, E. (1997) The crystal structure of dimeric kinesin and implications for microtubule-dependent motility. *Cell* **91**, 985–994
37. Vale, R.D. and Fletterick, R.J. (1997) The design plan of kinesin motors. *Annu. Rev. Cell Dev. Biol.* **13**, 745–777
38. Case, R.B., Rice, S., Hart, C.L., Ly, B., and Vale, R.D. (2000) Role of the kinesin neck linker and catalytic core in microtubule-based motility. *Curr. Biol.* **10**, 157–160
39. Seeger, M.A. and Rice, S.E. (2010) Microtubule-associated protein-like binding of the kinesin-1 tail to microtubules. *J. Biol. Chem.* **285**, 8155–8162
40. Maruta, S., Mizukura, Y., and Chaen, S. (2002) Interaction of a new fluorescent ATP analogue with skeletal muscle myosin subfragment-1. *J. Biochem.* **131**, 905–911
41. Maruta, S., Miyanishi, T., and Matsuda, G. (1989) Localization of the ATP-binding site in the 23-kDa and 20-kDa regions of the heavy chain of the skeletal muscle myosin head. *Eur. J. Biochem.* **184**, 213–221
42. Cross, R.A. (2004) The kinetic mechanism of kinesin. *Trends Biochem. Sci.* **29**, 301–309
43. Moyer, M.L., Gilbert, S.P., and Johnson, K.A. (1998) Pathway of ATP hydrolysis by monomeric and dimeric kinesin. *Biochemistry* **37**, 800–813
44. Ma, Y.Z. and Taylor, E.W. (1997) Kinetic mechanism of a monomeric kinesin construct. *J. Biol. Chem.* **272**, 717–723
45. Cochran, J.C., Krzysiak, T.C., and Gilbert, S.P. (2006) Pathway of ATP hydrolysis by monomeric kinesin Eg5. *Biochemistry* **45**, 12334–12344
46. Mackey, A.T. and Gilbert, S.P. (2000) Moving a microtubule may require two heads: a kinetic investigation of monomeric Ncd. *Biochemistry* **39**, 1346–1355
47. Moores, C.A. (2010) Kinesin-5 mitotic motors: is loop5 the on/off switch? *Cell Cycle* **9**, 1286–1290
48. Maliga, Z., Kapoor, T.M., and Mitchison, T.J. (2002) Evidence that monastrol is an allosteric inhibitor of the mitotic kinesin Eg5. *Chem. Biol.* **9**, 989–996
49. Song, Y.H., Marx, A., Müller, J., Woehlke, G., Schliwa, M., Krebs, A., Hoenger, A., and Mandelkow, E. (2001) Structure of a fast kinesin: implications for ATPase mechanism and interactions with microtubules. *EMBO J.* **20**, 6213–6225
50. Koo, B.S., Kalme, S., Yeo, S.H., Lee, S.J., and Yoon, M.Y. (2009) Molecular cloning and biochemical characterization of alpha- and beta-tubulin from potato plants (Solanum tuberosum L.). *Plant Physiol. Biochem.* **47**, 761–768
51. Mineyuki, Y. (2007) Plant microtubule studies: past and present. *J Plant Res.* **120**, 45–51
52. Sardar, H.S., Luczak, V.G., Lopez, M.M., Lister, B.C., and Gilbert, S.P. (2010) Mitotic kinesin CENP-E promotes microtubule plus-end elongation. *Curr Biol.* **20**, 1648–1653

Downloaded from http://jb.oxfordjournals.org/ at Changhua Christian Hospital on September 26, 2012